Available online at www.sciencedirect.com
SCIENCE DIRECT®
ELSEVIER
International Journal of Multiphase Flow 31 (2005) 1097–1115
International Journal of Multiphase Flow
www.elsevier.com/locate/ijmulflow

Modelling of dust lifting using the Lagrangian approach

Pawel Kosinski *, Alex C. Hoffmann

The University of Bergen, Department of Physics and Technology, Allegaten 55, 5007 Bergen, Norway

Received 15 June 2004; received in revised form 14 July 2005

Abstract

The subject of this paper is dust lifting behind shock waves, a process that is important for the formation of explosive dust clouds in air. While Eulerian–Eulerian has been the standard numerical technique for such simulations, the Eulerian–Lagrangian technique has been used in this paper, making it possible to take into account more physical phenomena, such as particle–particle and particle–wall collisions. The results of the simulations are shown mainly graphically, as snapshots of particle positions at given times after the passing of the shock wave. The results show that the collisions, and the coefficient of restitution assumed for them, is important in determining the mobility and lifting of dust behind shock waves. The results also show that the idea of a horizontally travelling shock wave is an oversimplification: the strong pressure gradient at the surface results in a series of reflected waves generated at the surface and travelling into the gas phase.

Keywords: Dust lifting; Explosion; Two-phase flow; Shock waves; Lagrangian model

1. Introduction

Dust lifting behind shock waves is a process that is especially interesting for engineers and researchers dealing with safety problems connected with dust explosions. Organic, metal or other

* Corresponding author. Tel.: +47 55 58 28 17; fax: +47 55 58 94 40.
E-mail address: pawel.kosinski@ift.uib.no (P. Kosinski).

0301-9322/$ - see front matter © 2005 Elsevier Ltd. All rights reserved.
doi:10.1016/j.ijmultiphaseflow.2005.07.003

kinds of dust can become hazardous when they are mixed with air and ignited. Such materials are present in many branches of industry and they constitute a potential danger for both people and equipment.

In practice dust is lying in deposits, for instance in processing units or in coal mines. The dust can easily be entrained by a pressure wave that may be generated intentionally or by accident. The latter case is unexpected and can lead to the creation of a dangerous mixture, and this type of occurrence has therefore been the subject of much research. Most of this research has been experimental, see for instance Fletcher (1976), Kauffman et al. (1992), Lebecki et al. (1995) and Lebecki et al. (2000). In those experiments a dust layer was lying at the lower wall of a channel and a primary explosion was generated with the object of creating a strong pressure wave. The wave propagated over the dust deposit and as a result the dust was entrained, dispersed and finally ignited.

This type of experiment is usually expensive and difficult to carry out, especially when accurate measurements are required. Therefore it has become popular to perform numerical simulations of such processes in recent years. One of the early studies was that of Butler et al. (1982) in which the interaction of a shock wave with a porous bed was modelled. The model used by Butler et al. was the basis of models used later by other researchers.

In the following years, other publications appeared, which were devoted specifically to the topic of the solid phase lifting behind a shock wave: Kuhl et al. (1989), Ben-Dor and Rayevsky (1991), Collins et al. (1994), Klemens et al. (2000), Thevand and Daniel (2002) and many others. The wider problem of modelling two-phase flows, with and without combustion, for safety applications have been a topic of many publications: Miura and Glass (1982), Dushin et al. (1993), Samuelsberg and Hjertager (1996), Boiko et al. (1997), Boiko and Poplavski (1997), Rose et al. (1997), Smirnov et al. (1997), Tu (1997), Mathiesen et al. (2000), Ibsen et al. (2000) and many others.

This paper is devoted to modelling dust lifting from a solid surface behind shock waves. In most of the publications mentioned above the main simulation method has been the so-called Eulerian approach, where the solid phase is treated as a continuum, penetrating and interacting with the gas phase and described by nearly the same equations as the gas phase. Both phases are coupled by a set of interphase interaction mechanisms, such as drag and lift force, heat and mass exchange and chemical reaction.

Not many attempts have been made to use the Lagrangian approach where the particles are treated as points that move in the computational domain interacting with the moving gas. Two-way coupling needs to be considered for this kind of process, since the particles act on the gas by changing its momentum significantly. Simulations using this approach are not easy to perform even nowadays due to the huge numbers of particles in real applications. On the positive side, this kind of simulation is very realistic from the physical point of view and many physical phenomena can be considered that cannot be accounted for in the Eulerian approach. An example is collisions between the particles: this is challenging and problematic for Eulerian models.

Summarizing: it is not possible to use the Lagrangian approach for simulation of dust lifting in large-scale domains covering real industrial facilities. However, using this approach for a smaller domain makes it possible to analyse the fundamental processes and seek the mechanisms responsible for entrainment of solid particles from a deposit.

2. Mathematical model

The model used here to describe the flow of the two-phase mixture can be divided into two parts. The first part is for simulation of the gas phase. The flow equations used are the Navier–Stokes equations, modified to take into account the presence of the solid particles, i.e. when modelling the exchange of momentum and heat between the gas and the particles, also the effect of the particles on the gas is taken into account (two-way coupling). Actually, there have been attempts in the literature to model the type of phenomena we are interested here neglecting this, only considering the action of the gas phase on the solid particles (one-way coupling). In such a case, the equations describing the movement are simply the Navier–Stokes equations. Using one-way coupling, however, has not been proven to be successful (see Thevand and Daniel, 2002).

The system of equations for the gas phase can be written in the following way:

$$\frac{\partial \rho}{\partial t} + \frac{\partial \rho u_{gj}}{\partial x_j} = 0 \tag{1}$$

$$\frac{\partial \rho u_{gi}}{\partial t} + \frac{\partial \rho u_{gj} u_{gi}}{\partial x_j} + \frac{\partial p}{\partial x_i} = \frac{\partial}{\partial x_j}\left(\rho \tau_{ji}\right) - f_i \tag{2}$$

$$\frac{\partial \rho E}{\partial t} + \frac{\partial \rho u_{gj}(E+p)}{\partial x_j} = \frac{\partial}{\partial x_j}\left(\rho u_{gi} \tau_{ij}\right) - Q + f_i u_{si} \tag{3}$$

$$\frac{p}{\rho} = R T_g \tag{4}$$

In the above: $\vec{u}_g$ is the velocity vector of the gas phase, ρ is the density of the gas phase, E is the total energy of the gas phase, p is the pressure in the gas phase, T_g is the temperature of the gas phase, τ_{ji} is the stress tensor, R is the universal gas constant, $\vec{f}$ is the force acting on the solid particles and Q is the heat exchanged between the gas phase and the particles.

The model for the solid particles can be written in the vector form as follows:

$$m_k \frac{\mathrm{d}\vec{u}_{sk}}{\mathrm{d}t} = \vec{f}_k \tag{5}$$

$$\frac{\mathrm{d}T_{sk}}{\mathrm{d}t} = \frac{1}{m_k c_s} Q_k \tag{6}$$

$$I_k \frac{\mathrm{d}\vec{\omega}_k}{\mathrm{d}t} = \vec{M}_k \tag{7}$$

and

$$k = 1, \ldots, \text{number of particles}$$

for the kth particle: m_k, I_k are the mass and moment; T_{sk} is the temperature; $\vec{u}_{sk}$ is the velocity; $\vec{\omega}_k$ is the angular velocity; $\vec{f}_k$ is the force acting on the particle due to interphase forces and collisions; Q_k is the heat exchange rate between the particle and the surrounding fluid; $\vec{M}_k$ is the torque acting on the particle due to collisions and due to shear stress on the particle surface; c_s is the heat capacity of the solid phase.

In the following, we describe how the force $\vec{f}_k$, torque $\vec{M}_k$ and rate of heat exchange Q_k are evaluated. Firstly the force acting on each particle as a result of the gas phase. This force mainly consists of the drag force:

$$\vec{f}_k = \vec{f}_{\text{drag}} = \frac{\pi d^2}{8} C_{\text{D}} \rho |\vec{u}_{\text{g}} - \vec{u}_{\text{s}}| (\vec{u}_{\text{g}} - \vec{u}_{\text{s}}) \tag{8}$$

where d is the particle diameter (constant for all the particles, but different diameters could easily be implemented) and C_{D} is the drag force coefficient (a function of the Reynolds number).

The force $\vec{f}_k$ is related to $\vec{f}$ (used in (2) and (3)) as:

$$\vec{f} = n\vec{f}_k$$

where n is a number density of the particle phase.

We have to emphasize that other interphase forces can be also included in the modelling, we discuss this below.

The torque due to the shear stress acting on the particle by the fluid can be described for the following model (Crowe et al., 1998):

- for low Reynolds numbers (Happel and Brenner, 1973):

$$\vec{M}_k = \pi \mu d^3 (1/2 \nabla \times \vec{u}_{\text{g}} - \vec{\omega}_k) \tag{9}$$

- for higher Reynolds numbers (Denis et al., 1980):

$$\vec{M}_k = -2.01 \mu d^3 \vec{\omega}_k (1 + 0.201 \sqrt{Re_\omega}) \tag{10}$$

where Re_ω is a Reynolds number based on the angular velocity:

$$Re_\omega = \frac{\rho \mid \vec{\omega}_k \mid d^2}{4\mu} \tag{11}$$

and μ is the dynamic viscosity of the gas phase.

Additionally, the force acting on each particle is also a result of collisions with other particles.

For modelling of the collisions, the so-called hard sphere model has been adopted. Its detailed description for the three-dimensional case may be found, for example, in Crowe et al. (1998). The derivation of the model begins with writing the impulse equations for both colliding particles, denoted by subscripts A and B. Symbol (0) refers to the state before the collision:

$$m_{\text{A}}(u_{\text{A}} - u_{\text{A}}^{(0)}) = J_X \tag{12}$$

$$m_{\text{A}}(v_{\text{A}} - v_{\text{A}}^{(0)}) = J_Y \tag{13}$$

$$m_{\text{B}}(u_{\text{B}} - u_{\text{B}}^{(0)}) = -J_X \tag{14}$$

$$m_{\text{B}}(v_{\text{B}} - v_{\text{B}}^{(0)}) = -J_Y \tag{15}$$

$$I_{\text{A}}(\omega_{\text{A}} - \omega_{\text{A}}^{(0)}) = d_{\text{A}}/2 \cdot (\vec{n} \times \vec{J})_Z \tag{16}$$

$$I_{\text{B}}(\omega_{\text{B}} - \omega_{\text{B}}^{(0)}) = d_{\text{B}}/2 \cdot (\vec{n} \times \vec{J})_Z \tag{17}$$

In the above: I_A is the moment of inertia of a particle (for spherical particles: $I = (1/10)md^2$); $\vec{J}$ is the impulsive force (the time integral of the force throughout the collision) exerted on particle A (which also acts on the B, but with the opposite sign); $\vec{n}$ is a unit normal vector from particle A to B; $(\vec{n} \times \vec{J})_z$ is the z-component of the vector product of the normal vector and the impulsive force, and m is mass of a particle.

In the model (15)–(20) the particle deformation is neglected, and it is assumed that the friction on sliding particles obeys Coulombs law. This is described by a constant friction coefficient μ_e. Additionally a coefficient of restitution e is defined as the ratio of the post-collisional to the pre-collisional velocities normal to $\vec{n}$. The coefficient is taken as constant. The integration of the equations with the mentioned assumptions leads to values of velocities and rotations for the both particles after the collision. Detailed formulae can be found in Crowe et al. (1998).

Heat transfer between the gas phase and the particles takes place due to a difference of temperatures between them. In this research only convective flux has been considered and modelled using the well known formula:

$$Q_k = \pi d \lambda Nu (T_g - T_s) \tag{18}$$

where λ is the conductivity of the gas phase and Nu is the Nusselt number (an empirical function of Reynolds and Prandtl numbers).

The value Q_k is related to Q (used in (3)) as:

$$Q = nQ_k$$

where n is a number density of the particle phase.

The number of equations of conservation corresponds to the number of the particles. Using huge numbers of particles is not feasible due to the limited memory of a computer. One of the methods of overcoming this problem and increase the number of particles in the system is to consider "virtual particles" that each consists of a number of primary particles. The problem is that it may lead to errors when studying phenomena of dust lifting, especially for thin layers. If this technique were used, it would not be possible to analyse the fundamental processes taking place in the layer. Therefore this technique has not been used in the present research.

3. Computational technique

As described in the previous section, the following problems must be considered in the algorithm:

- the flow of the gas phase,
- the motion of the particles as a result of interphase forces,
- the motion of the particles as a result of collisions.

3.1. The flow of the gas phase

The system of equations for the gas phase (1)–(3) can be written in the following way (for the two-dimensional case):

$$\frac{\partial \overline{U}}{\partial t}+\frac{\partial(\overline{F}-\overline{F}_V)}{\partial x}+\frac{\partial(\overline{G}-\overline{G}_V)}{\partial y}=\overline{S} \tag{19}$$

where: $\overline{U},\overline{F},\overline{G},\overline{F}_V,\overline{G}_V$ are vectors:

$\overline{U}$ is the vector of conserved variables; $\overline{F},\overline{G}$ are the vectors containing convective fluxes through cell edges; $\overline{F}_V,\overline{G}_V$ is the vector containing diffusive fluxes through cell edges; $\overline{S}$ is the vector containing source terms:

$$\overline{U}=\begin{bmatrix}\rho\\ \rho u_g\\ \rho v_g\\ \rho E\end{bmatrix};\quad \overline{F}=\begin{bmatrix}\rho u_g\\ \rho u_g^2+p\\ \rho u_g v_g\\ \rho u_g(E+p)\end{bmatrix};\quad \overline{G}=\begin{bmatrix}\rho v_g\\ \rho u_g v_g\\ \rho v_g^2+p\\ \rho v_g(E+p)\end{bmatrix};$$

$$\overline{F}_V=\begin{bmatrix}0\\ \rho\tau_{xx}\\ \rho\tau_{yx}\\ \rho u_g\tau_{xx}+\rho v_g\tau_{xy}\end{bmatrix};\quad \overline{G}_V=\begin{bmatrix}0\\ \rho\tau_{xy}\\ \rho\tau_{yy}\\ \rho u_g\tau_{yx}+\rho v_g\tau_{yy}\end{bmatrix};\quad \overline{S}=\begin{bmatrix}0\\ f_x\\ f_y\\ Q+f_x u_s+f_y v_s\end{bmatrix} \tag{20}$$

In (20) the following notation has been used: u_g and v_g are components of the gas phase velocity in x- and y-direction; u_s and v_s are components of the solid phase velocity. The dimensions of the vectors in (19) and (20) correspond to the number of equations of conservation. For two-dimensional flow we thus obtain four such equations.

The computational grid has been divided into $nx\times ny$ rectangular elements. The values of the gas parameters (density, velocity components, pressure and temperature) are written in the cell centres. The parameters of all the particles (position, velocities, temperature) are stored. In each time step the new values of gas and particle properties in the cells are calculated using numerical techniques mentioned below.

The total scheme of the algorithm is based on the idea of splitting (see Toro, 1999), where the Eq. (19) are solved separately:

- the flow of the gas phase where interphase mechanisms are not considered:

$$\frac{\partial \overline{U}}{\partial t}+\frac{\partial(\overline{F}-\overline{F}_V)}{\partial x}+\frac{\partial(\overline{G}-\overline{G}_V)}{\partial y}=\overline{0} \tag{21}$$

- the change in time of the conserved variables as a result of particles motion and temperature difference:

$$\frac{\partial \overline{U}}{\partial t}=S(\overline{U}) \tag{22}$$

The numerical scheme for solving (21) begins with writing the equations in the following way (see e.g. Toro, 1999):

$$\overline{U}_j^{n+1} = \overline{U}_j^n + \frac{\Delta t}{\Delta x}\left[\left(\overline{F}_{j-\frac{1}{2},k} - \overline{F}_{V\,j-\frac{1}{2},k}\right) - \left(\overline{F}_{j+\frac{1}{2},j} - \overline{F}_{V\,j+\frac{1}{2},k}\right)\right] + \frac{\Delta t}{\Delta y}\left[\left(\overline{G}_{j,k-\frac{1}{2}} - \overline{G}_{V\,j,k-\frac{1}{2}}\right) - \left(\overline{G}_{j,k+\frac{1}{2}} - \overline{G}_{V\,j,k+\frac{1}{2}}\right)\right] \tag{23}$$

for $j = 1,\ldots,nx$; $k = 1,\ldots,nz$; and n indicates the time step.

In the scheme $\overline{F}$, $\overline{G}$ (defined above in (20)) constitute fluxes. Their values at the cell interfaces are based on solving the Riemann problem between two adjacent cells, a problem is well known in gas dynamics. Here the Godunov-type MUSCL Hancock (van Leer) partial differential solver was used, so that the second-order spatial accuracy was obtained. The main advantage of using this method is the possibility of resolving high gradients and discontinuities typical for high-speed flows and shock waves.

The vectors $\overline{F}_V$, $\overline{G}_V$ are diffusive fluxes and also have been defined above, in (20). In the numerical scheme they are written in a simple finite difference manner using parameters from adjacent computational cells.

In the next step Eq. (22) is solved. They constitute a system of ordinary differential equations. The part of the algorithm involves solving equations of motion of the solid particles as a result of the interphase mechanisms. It is described in the following section.

3.2. The motion of the particles as a result of interphase mechanisms

In order to solve the motion of the particles on the computational grid, Eqs. (5)–(7) must be considered. They constitute a system of ordinary differential equations. Because of they can be solved together with the system (22) as mentioned above. It has been performed by using the VODE solver (see Kee et al., 1996) that is a high-order implicit scheme widely used for solving these kinds of equations. Altogether there are seven equations and the following parameters are found in the new time step: two components of the corrected gas velocity, two components of a particle velocity, temperatures of the both phases and angular velocity of a particle. Having done this, the new position of a particle is found as a function of its previous position, as well as new and previous velocities.

$$x_i^{n+1} = x_i^n + \Delta t\frac{u_{si}^{n+1} + u_{si}^{n+1}}{2}$$
$$y_i^{n+1} = y_i^n + \Delta t\frac{v_{si}^{n+1} + v_{si}^{n+1}}{2} \tag{24}$$

The procedure for solving the ordinary differential equations, described in this section, is called for each particle separately. The parameters of the particles are stored for all of them individually. Moreover, during the computation of the interphase mechanisms, it is required to find the values of gas parameters around each of them. Because the gas parameters are stored in the cells centres, it is necessary to perform an interpolation to assess the exact values of the gas parameters.

3.3. The collisions between the particles

A part of the algorithm is the collision between the particles. At the beginning of performing the calculations for each time step all the pairs of particles that collide in the current time step are

taken into account. It is done by analysis of the distance between them. If, within the time step, the distance becomes smaller or equal than the sum of radii of the particles they will collide. Having done this, their new parameters are found and new values of velocities (both linear and angular) of the particles are introduced by implementing the analytical formulae mentioned above.

3.4. The sequence

The idea of the algorithm is to find the gas and the particles parameters in the new time step. In each time step the algorithm solves all the three parts described in Sections 3.1–3.3. They can be denoted using the following operators:

Φ—the flow of the gas phase in x- and y-direction (Section 3.1);
Λ—the computation of the interphase mechanisms and of new parameters of the particles and the gas phase as a result of them (Section 3.2);
Γ—the movement of the particles as a result of collisions (Section 3.3).

In the algorithm they are solved in the following sequence:

$$\overline{U}^n \rightarrow \Lambda^{(1/2\Delta t)} \rightarrow \Gamma^{(1/2\Delta t)} \rightarrow \Phi^{(\Delta t)} \rightarrow \Gamma^{(1/2\Delta t)} \rightarrow \Lambda^{(1/2\Delta t)} \rightarrow \overline{U}^{n+1} \tag{25}$$

where: $\overline{U}^n$ is the parameters in the previous time step; $\Lambda^{(1/2\Delta t)}$ is the computation of the interphase mechanism for half of the time step; $\Gamma^{(1/2\Delta t)}$ is the computation of new particle velocities after collision (in half of the time step); $\Phi^{(\Delta t)}$ is the flow of the gas phase for full time step; $\overline{U}^{n+1}$ is the parameters in the new time step.

4. Results

The simulations are two-dimensional and were performed on a rectangular domain whose dimensions are: 40 cm per 1 cm (Fig. 1). The walls of the channel were modelled as being open so that no obstructions were present to the flowing gas and no unexpected pressure waves were created. The main shock wave was created by a high-pressure chamber. At $t = 0$ an impenetrable membrane in front of the chamber was removed exposing the computational domain to the

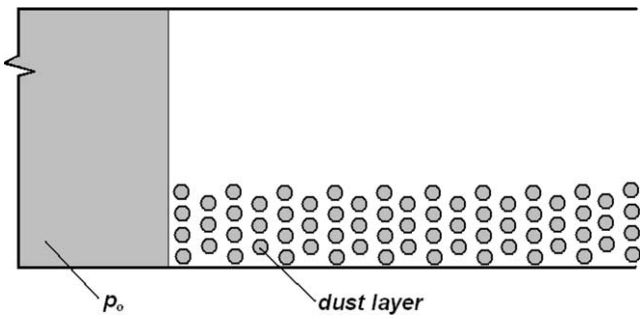

Fig. 1. The scheme of the computational domain.

pressure in the chamber, resulting in a shock wave travelling through the domain and passing over the deposit that had been situated initially at the lower side of the channel. The gas pressure in the chamber was 4 bar. The solid particles, whose diameter was equal to 90 μm, were spherical and were initially lying in the configuration presented in Fig. 1. This initial configuration was kept the same in all the simulations.

The most important parameter that was varied between the numerical experiments was the collision restitution coefficient. The objective was to investigate the importance of the collisions between the particles and the collisions of the particles with the lower wall of the channel.

Convergence studies are of importance, especially when a two-way coupling technique is used (both the influence of the gas on the particles and of the particles on the gas are considered). When

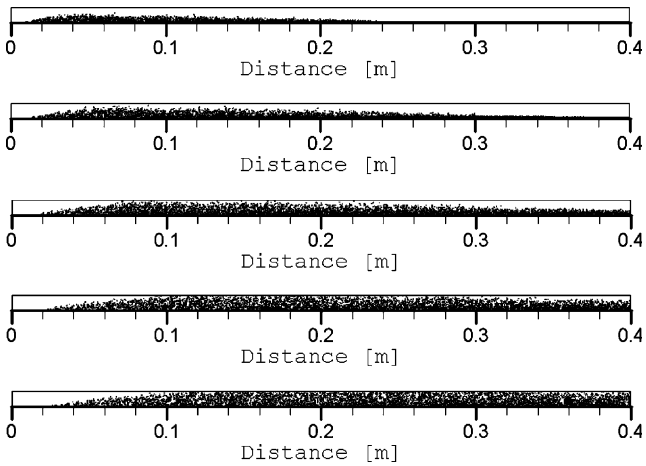

Fig. 2. The particles distribution for the restitution coefficient equal to 0.9. Results are presented for five moments of time: 1.0, 1.3, 1.6, 1.9 and 2.2 ms.

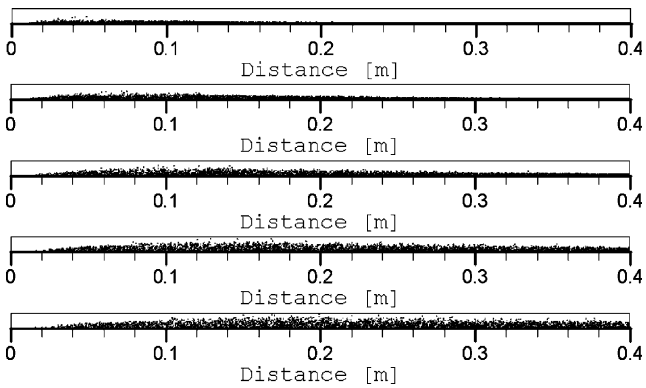

Fig. 3. The particles distribution for the restitution coefficient equal to 0.3. Results are presented for five moments of time: 1.0, 1.3, 1.6, 1.9 and 2.2 ms.

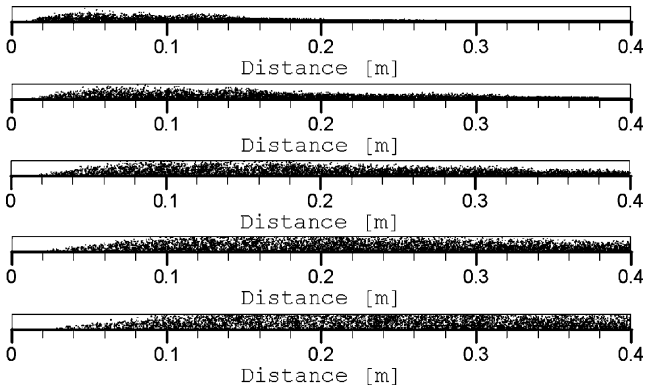

Fig. 4. The particles distribution for the restitution coefficient equal to 1.0 and the friction coefficient 0.0. Results are presented for five moments of time: 1.0, 1.3, 1.6, 1.9 and 2.2 ms.

the influence of the particles on the behaviour of the gas phase can be neglected (one-way coupling), the results are less grid-dependent (see e.g. Portela and Oliemans, 2003). In this research,

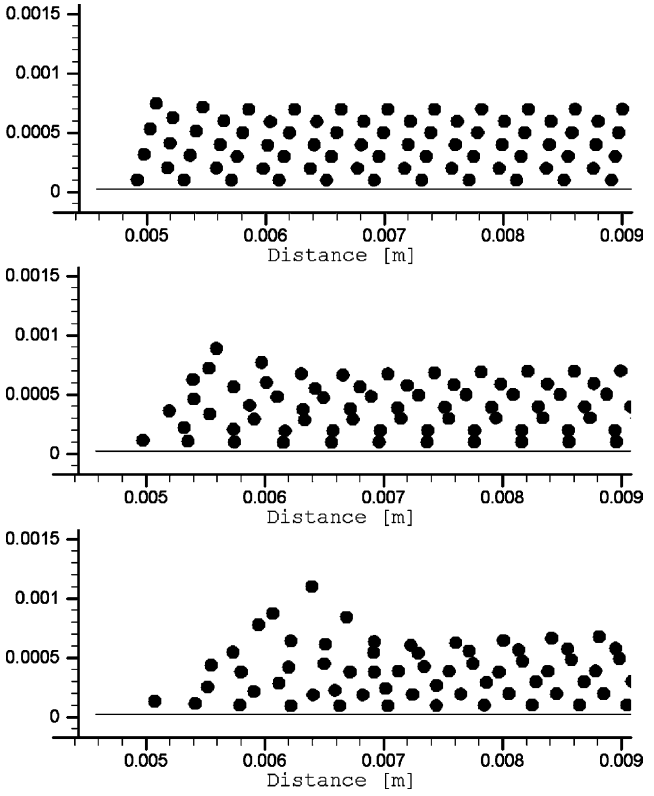

Fig. 5. The particles distribution for the restitution coefficient equal to 0.9 and the friction coefficient 0.15. Results are presented for five moments of time: 0.05, 0.10 and 0.15 ms.

the results were tested by checking convergence on different meshes corresponding to the following sizes of the (square) cells: 200, 400 and 800 μm. It must be noted here that too fine grids do not describe reality correctly, since the diameter of the particles then becomes large in comparison with the cell size. This problem can be overcome by implementing the particles not as points but as objects, large relative to the computational cells and moving on the grid. This requires significant amendments in the numerical scheme. We are working on this aspect now.

In this research, during the convergence studies snapshots of the particle locations for the different grids mentioned above were compared. Additionally, so-called mean square displacement of the particles for a time t was computed for different grids and the histories of this function were analysed. Finally pressure histories at different points in the channel were investigated. On this basis, the grid corresponding to 200 μm was chosen as optimal.

Figures 2–4 show the particles' distribution for different moments in time after the passing of the shock wave and for different restitution coefficients. The points in time are 1.0, 1.3, 1.6, 1.9 and 2.2 ms for all the three values of the restitution coefficient which are 0.9, 0.3 and 1.0 for Figs. 2–4, respectively. The friction coefficient was equal to 0.15. The last case describes an ideal situation where the collisions are fully elastic. In this case the value of the friction coefficient also corresponded to an ideal case and was equal to 0.0.

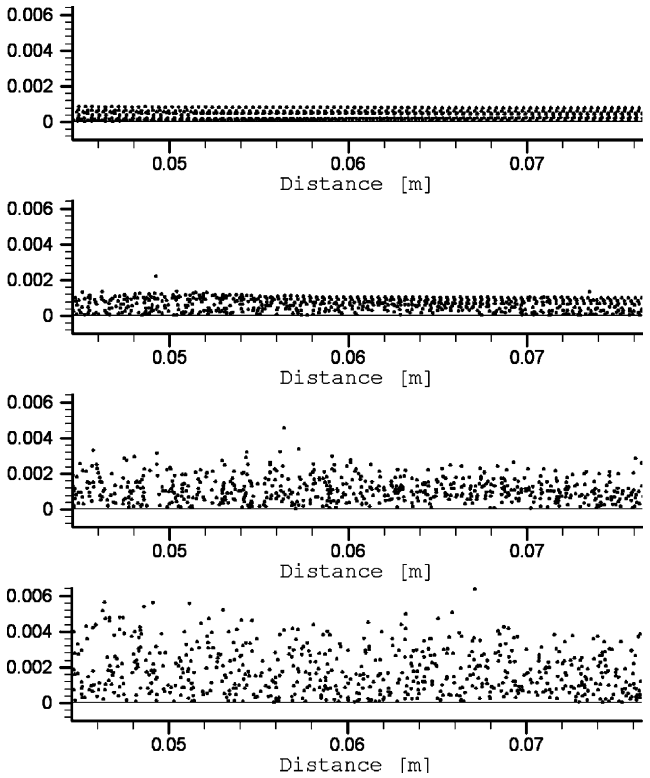

Fig. 6. The particles distribution for the restitution coefficient equal to 0.9 and the friction coefficient 0.15. Results are presented for three moments of time: 0.4, 0.6, 0.8 and 1.0 ms.

Comparison of the results leads to an interesting conclusion: a lower restitution coefficient slows down the entrainment process. This means that the effect of collisions on the phenomena is of importance. According to some experiments (e.g. Goldschmidt et al., 2001), the value of coefficient of restitution for such particles is usually close to 0.9. Thus the results obtained with this value can be expected to be closer to reality.

As seen in e.g. Figs. 2–4, the following trend can be observed: the particles are lifted in a wedge-like shape and later begin to move randomly due to frequent interparticle collisions. The same trend was observed during experimental investigations of dust lifting behind shock waves (see e.g. Klemens et al., 2004; Borisov et al., 1999).

In the following, the fundamental phenomena present in the layer are discussed.

Figure 5 shows details of the front part of the layer during the initial stages of the process (0.05; 0.10; and 0.15 ms) where the shock wave hits the layering and leads to the lifting of the first particles. The results are shown for the value of the restitution coefficient 0.9 and the friction coefficient 0.15, but the collisions between the particles are negligible at this stage, and the lifting process is a only result of the upwards gas flow. It is noted that the Eulerian–Eulerian approach is able to model the phenomenon in a similar way, since the particle–particle interactions can, to some extent, be neglected at this stage.

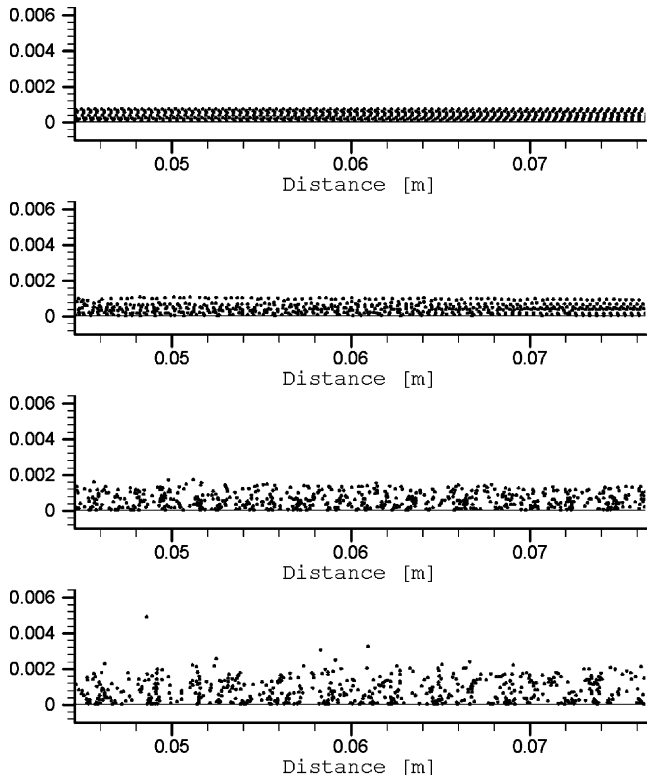

Fig. 7. The particles distribution for the restitution coefficient equal to 0.3 and the friction coefficient 0.15. Results are presented for three moments of time: 0.4, 0.6, 0.8 and 1.0 ms.

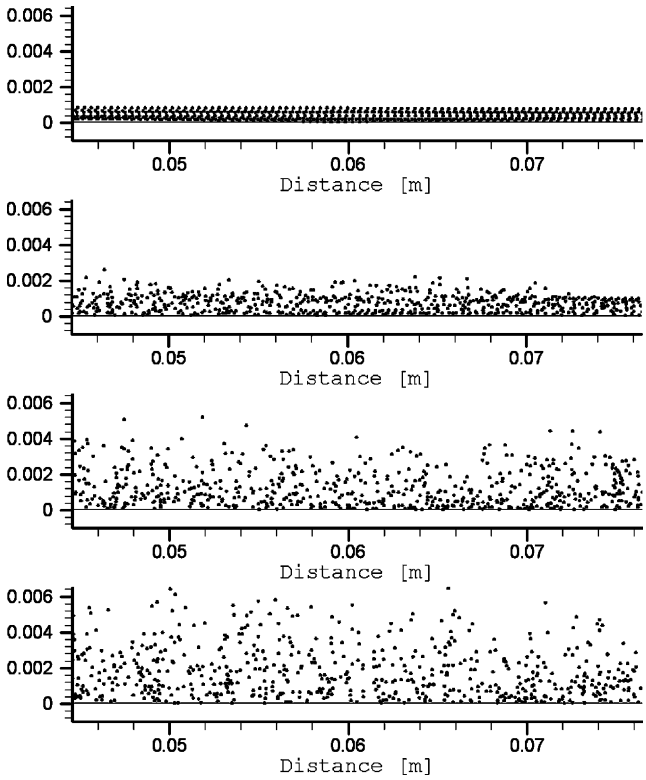

Fig. 8. The particles distribution for the restitution coefficient equal to 1.0 and the friction coefficient 0.0. Results are presented for three moments of time: 0.4, 0.6, 0.8 and 1.0 ms.

Figures 6–8 present the particle distributions for three moments in time: 0.4, 0.6, 0.8 and 1.0 ms for restitution coefficients 0.9, 0.3 and 1.0, respectively. As previously, the friction coefficient was equal to 0.15 for the first two cases and 0.3 for the third case. The difference between Figs. 6–8 and Figs. 2–4 is that in the latter the domain where the main lifting process occurs is magnified, so that the process can be better investigated. The first conclusion is again that the higher value of the restitution coefficient, the stronger lifting process. The lifting process begins when the particles in the deposit come to contact with each other and bounce. Afterwards, the chaotic movement and collisions with the particles carried by the gas stream from the left lead to a behaviour difficult to predict. However, the particles are moving quickly in the vertical direction.

The domain has been even more magnified in Figs. 9–11. The figures correspond to the same cases as in Figs. 6–8, and Figs. 2–4. We can observe all the processes that occur within the layer: the gas movement causes the particles come into contact and collide. An important remark is that that the entrainment does not occur directly after the passing of the shockwave, but only delayed, after collisional processes in the layer have taken place. It must be emphasized that a similar delay has been reported in experiments (see e.g. Fletcher, 1976; Klemens et al., 2004) but it has not been explained up to now.

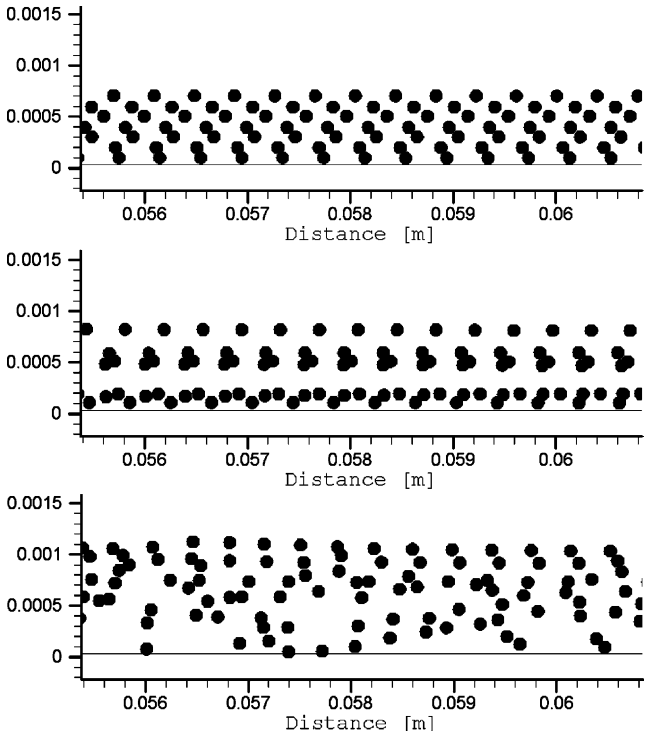

Fig. 9. The particles distribution for the restitution coefficient equal to 0.9 and the friction coefficient 0.15. Results are presented for three moments of time: 0.2, 0.4 and 0.6 ms.

Figure 12 compares the particle–particle interactions for the two cases: the coefficient of restitution 0.9 and 0.3. It can be observed that for the lower value of the coefficient, the particles tend to stick to each other more easily and they may form agglomerates. A similar conclusion has been drawn by other researchers, dealing with fluidized beds.

Another interesting phenomenon, which these simulations have brought to light, is the fact that the shock wave is not one-dimensional, and that waves are periodically reflected into the domain from the lower wall. The reflection of the waves is caused by the fact that the main shock wave is not straight but curved due to the presence of the dust. This is shown in Fig. 13 as a pressure distribution in the vicinity of the shock wave. Similar results were obtained by e.g. Collins et al. (1994) who used the Eulerian approach.

The last problem that has been considered in the present work was an artificial case where no actual collisions between the particles were modelled. In this unreal situation, the particles were allowed to pass through each other. In the computer programme it was realized by switching off the procedures responsible for the collisions.

The results are presented in Fig. 14. Comparing them to the results from Figs. 2–4, it is easily observed that the lifting process in not intense and does not correspond to reality. We note that most researchers, who used the Eulerian–Eulerian approach, have obtained virtually the same results as the ones shown in Fig. 14.

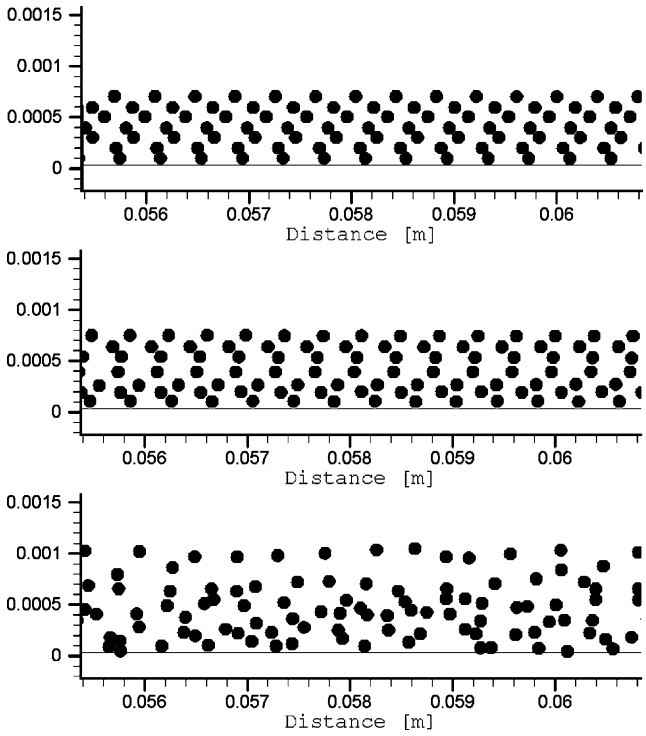

Fig. 10. The particles distribution for the restitution coefficient equal to 0.3 and the friction coefficient 0.15. Results are presented for three moments of time: 0.2, 0.4 and 0.6 ms.

5. Concluding remarks

This paper has been devoted to the problems of modelling dust lifting. The Lagrangian approach has been adopted, which has not been used for modelling such processes so far. However, the growth in computer power makes it possible to begin using the technique as a supplement to the traditional Eulerian technique. The main advantage of the Lagrangian approach is the possibility of implementing many physical phenomena so that the process of dust entrainment can be thoroughly investigated. In this paper the influence of collisions between the particles has been considered. It has been shown that these phenomena change the process significantly and they cannot be neglected.

It must be noted that the dust layer was modelled using the special configuration presented in Fig. 1. The configuration does not correspond directly to reality where the particles are in contact from the very beginning and they are placed chaotically. In our research we limited ourselves to investigating and proving the importance of the effect of collisions and therefore we stayed with this configuration. Specifically our simulations do not yet account for the effect of particle–particle and particle–wall adhesion, either in preventing the dispersion of the layer in the first place or in forming agglomerates below a lower impact threshold. In subsequent work we wish to address these issues and study how the initial configuration of the dust particles influences the process.

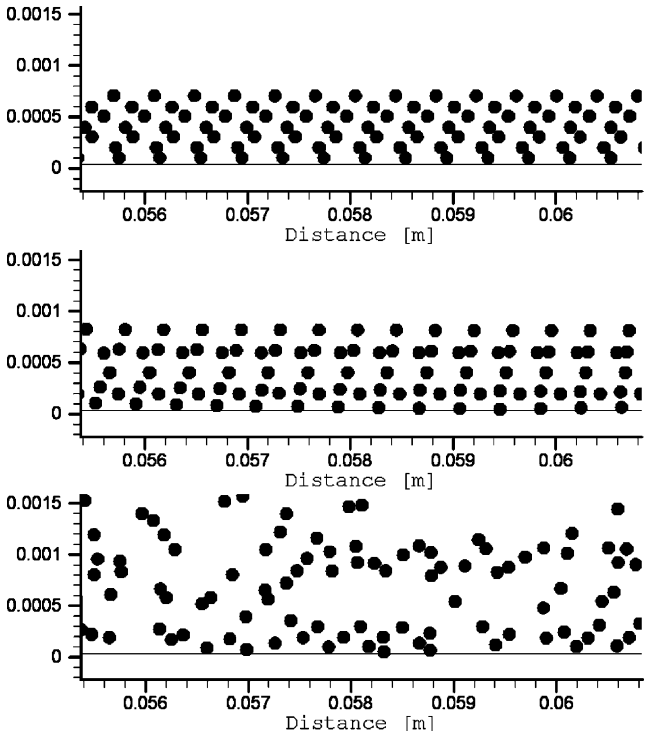

Fig. 11. The particles distribution for the restitution coefficient equal to 1.0 and the friction coefficient 0.0. Results are presented for three moments of time: 0.2, 0.4 and 0.6 ms.

In this paper the results from two-dimensional simulations are presented. If a three-dimensional case were considered, additional effect could have been modelled: particle/turbulence interaction, complex interactions between the particles, as well as interactions with two additional walls. Portela and Oliemans (2003) analyse a similar problem: dispersion of particles and their deposition and re-suspension at the walls. They obtain stream-wise vortices close to the wall, a phenomenon responsible for behaviour of particles in the near-wall region. Their research, however, is limited to low-velocity regimes, and no particle/particle interactions were considered. In our paper, on the other hand, the gas flow is mainly one-dimensional with high velocity and we are interested in solving the following problem: are the particle/particle and particle/wall interactions important or not for simulating the particle entrainment process? For this, a two-dimensional simulation is sufficient and most researchers working in this field used the same strategy: Kuhl et al. (1989), Ben-Dor and Rayevsky (1991), Collins et al. (1994), Klemens et al. (2000), Thevand and Daniel (2002). In fact in our previous works we have made an attempt of simulating the problem using the Eulerian–Eulerian technique (less time consuming) for three-dimensional geometry. This led to results that are only slightly different from Eulerian–Eulerian simulations in two dimensions.

Another phenomenon, which we have not yet accounted for, is fluid-dynamical lift forces on the particles. The Lagrangian approach is, in principle, suitable for taking this into account, and we

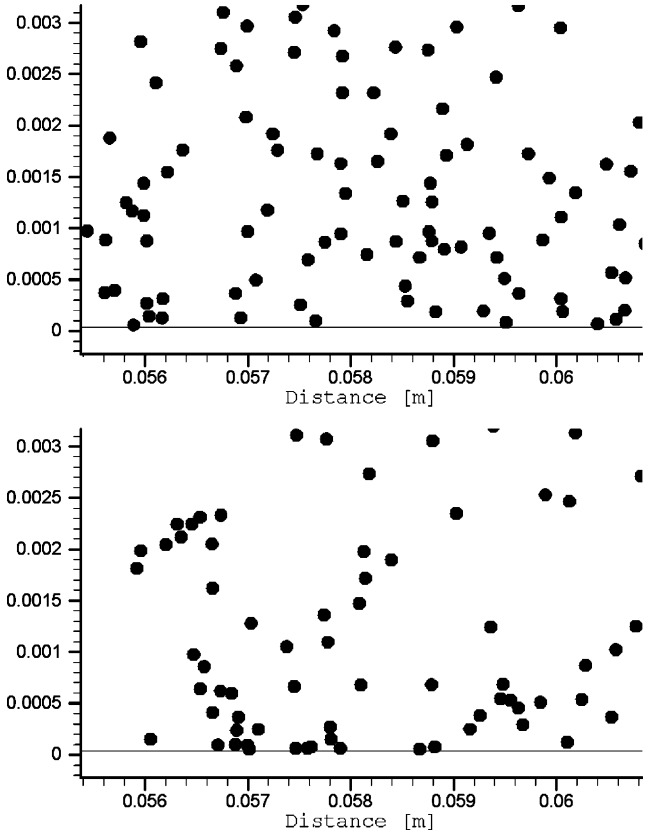

Fig. 12. The particles distribution for the moment of time 1.0 ms and for two restitution coefficients: 0.9 and 0.3. The friction coefficient is equal to 0.15.

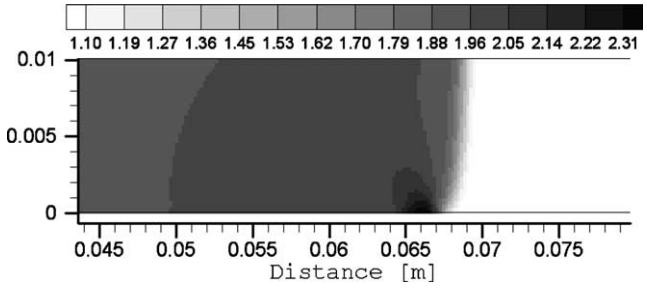

Fig. 13. The pressure [bar] distribution in the vicinity of the shock wave after 0.15 ms.

wish to do so in subsequent work. Initial simulations show interesting effects when including the effects of the Saffman and Magnus forces on the particles.

According to this research the following mechanisms are important for dust lifting behind a shock wave. There are instabilities in the layer when a shock wave passes over and through it,

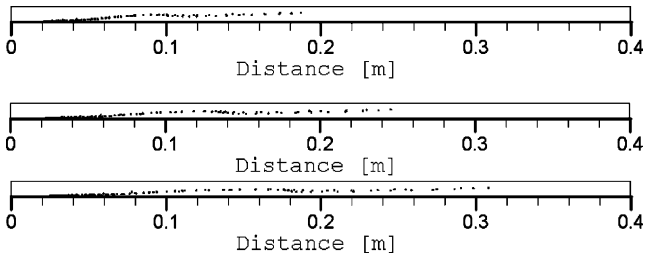

Fig. 14. The particles distribution for three moments of time: 2.5, 3.0 and 3.5 ms. The collisions between the particles have not been included.

and collisions between the particles lead to the chaotic movement of them in every direction. These effects can be amplified by the existence of lifting forces that are functions of rotation of the particles and the gas around them (not considered in this research).

The simulations have been performed on a relatively small computational domain. It will be interesting and important to repeat the modelling for bigger channels so that it can be checked how the process develops.

Acknowledgement

The authors would like to thank Prof. Rudolf Klemens (Warsaw University of Technology) for interesting discussions regarding experimental results of dust lifting behind shock wave. Also we should express our gratitude to Prof. Rolf Eckhoff and Dr. Bjorn Arntzen (The University of Bergen) for useful remarks about the modelling these phenomena.

References

Ben-Dor, G., Rayevsky, D., 1991. Shock wave interaction with a dense gas layer. In: Proceedings of International Workshop on Strong Shock Waves. pp. 145–163.

Boiko, V.M., Poplavski, S.V., 1997. On the effect of particles concentration on acceleration of a dusty cloud behind the shock wave. Archivum Combustionis 17, 19–26.

Boiko, V.M., Kiselev, V.P., Kiselev, S.P., Papyrin, A.N., Poplavsky, S.V., Fomin, V.M., 1997. Shock wave interaction with a cloud of particles. Shock Waves 7, 275–285.

Borisov, A.A., Sumskoi, S.I., Komissarov, P.V., 1999. Experimental and numerical modelling of shock wave interaction with a dust layer. In: Proceedings of the 17th International Colloquium on the Dynamics of Explosions and Reactive Systems.

Butler, P.B., Lembeck, M.F., Krier, H., 1982. Modelling of shock development and transition to detonation initiated by burning in porous propellant beds. Combustion and Flame 46, 75–94.

Collins, J.P., Fergusson, J.P., Chien, K.Y., Kuhl, A.L., Krispin, J., Glaz, H.M., 1994. Simulation of shock-induced dusty gas flows using various models. In: Proceedings of 25th AIAA Fluid Dynamics Conference, AIAA-1994-2309.

Crowe, C., Sommerfeld, M., Tsuji, Y., 1998. Multiphase Flows with Droplets and Particles. CRC Press LLC.

Denis, S.C.R., Singh, S.N., Ingham, D.B., 1980. The steady flow due to a rotating sphere at low and moderate Reynolds numbers. J. Fluid Mech. 101, 257–279.

Dushin, V.R., Nikitin, V.F., Smirnov, N.N., Zverev, N.I., Machviladze, G.M., Yakush, S.E., 1993. Mathematical modelling of particle cloud evolution in the atmosphere after a huge explosion. In: Proceedings of the 5th International Colloquium on Dust Explosions. pp. 287–292.

Fletcher, B., 1976. The interaction of a shock with a dust deposit. J. Phy. D: Appl. Phys. 9, 197–202.

Goldschmidt, M.J.V., Kuipers, J.A.M., Van Swaaij, W.P.M., 2001. Hydrodynamic modelling of dense gas-fluidised beds using the kinetic theory of granular flow: effect of coefficient of restitution on bed dynamics. Chem. Eng. Sci. 56, 571–578.

Happel, J., Brenner, H., 1973. Low Reynolds Number Hydrodynamics. Noordhoff Intl. Pub., Leiden.

Ibsen, C.H., Solberg, T., Hjertager, B.H., 2000. The influence of the number of phases in Eulerian multiphase simulations. In: Proceedings of the 14th International Congress of Chemical and Process Engineering. pp. 27–31.

Kauffman, C.W., Sichel, M., Wolanski, P., 1992. Research on dust explosions at the University of Michigan. Powder Technol. 71, 119–134.

Kee, R.J., Rupley, F.M., Meeks, E., 1996. Chemkin-III: A Fortran Chemical Kinetics Package for the Analysis of Gas-Phase Chemical and Plasma Kinetics, SAND96-8216.

Klemens, R., Kosinski, P., Wolanski, P., Korobeinikov, V.P., Markov, V.V., Menshov, I.S., Semenov, I.V., 2000. Numerical modelling of coal mine explosion. In: Proceedings of the Third International Symposium on Hazards, Prevention, and Mitigation of Industrial Explosions. pp. 103–108.

Klemens, R., Zydak, P., Kaluzny, M., Litwin, D., Wolanski, P., 2004. Mechanism of dust dispersion from the layer by propagating shock wave in the flow without obstacles. In: Proceedings of the Fifth International Symposium on Hazards, Prevention and Mitigation of Industrial Explosions.

Kuhl, A.L., Chien, K.Y., Fergusson, R.E., Glowacki, W.J., Collins, P., Glaz, H.M., Colella, P., 1989. Dust scouring by a turbulent boundary layer behind a shock. Archivum Combustionis 9, 40–53.

Lebecki, K., Cybulski, K., Sliz, J., Dyduch, Z., Wolanski, P., 1995. Large scale grain dust explosions-research in Poland. Shock Waves 5, 109–114.

Lebecki, K., Oli, J., Cybulski, K., Dyduch, Z., 2000. Efficiency of trigerred barriers in dust explosion suppression in galleries. In: Proceedings of the Third International Symposium on Hazards, Prevention, and Mitigation of Industrial Explosions. pp. 66–73.

Mathiesen, V., Solberg, T., Hjertager, B.H., 2000. An experimental and computational study of multiphase flow behaviour in a circulating fluidised bed. Int. J. Multiphase Flow 26, 387–419.

Miura, H., Glass, I.I., 1982. On a dusty-gas shock tube. Proc. Roy. Soc. London Series A: Math. Phys. Eng. Sci. 382, 373–388.

Portela, L.M., Oliemans, R.V.A., 2003. Eulerian–Lagrangian DNS/LES of particle–turbulence interactions in wall-bounded flows. Int. J. Numer. Meth. Fluids 43, 1045–1065.

Rose, M., Roth, P., Frolov, S.M., Neuhaus, M.G., Klemens, R., 1997. Lagrangian Approach for Modelling Two-phase Turbulent Reactive Flows. Advanced Computation and Analysis of Combustion. ENAS Publishers, pp. 175–194.

Samuelsberg, A., Hjertager, B.H., 1996. An experimental and numerical study of flow patterns in a circulating fluidized bed reactor. Int. J. Multiphase Flow 22, 575–591.

Smirnov, N.N., Nikitin, V.F., Legros, J.C., 1997. Turbulent Combustion of Multiphase Gas-Particles Mixtures. Thermogravitational Instability. Advanced Computation and Analysis of Combustion. ENAS Publishers, pp. 136–160.

Thevand, N., Daniel, E., 2002. Numerical study of the lift force influence on two-phase shock tube boundary layer characteristics. Shock Waves 11, 279–288.

Toro, E.F., 1999. Riemann Solvers and Numerical Methods for Fluid Dynamics. A Practical Introduction. Springer-Verlag.

Tu, J.Y., 1997. Computation of turbulent two-phase flow on overlapped grids. Numer. Heat Transfer 32, 175–195.